

Autonomous Control of Small Satellite Formations using Differential Drag

Daniel Groesbeck *
Georgia Institute of Technology, Atlanta, GA, 30332

This study develops a methodology for the autonomous control of multiple small satellites, to include CubeSats, designed to operate in a formation or constellation in Low Earth Orbit (LEO). The satellites are assumed to have no onboard propellant and will rely solely on changing the orientations of the satellites, creating a differential drag force that will be the control mechanism. The control systems that were developed account for the reduction of inter-satellite distance drift and maneuver controls such that two satellites could change the mean relative distance between them while not imparting an additional drift rate. These systems were developed on the assumption of identical satellites operating in similar, near circular coplanar orbits. Simulations were run to validate the functionality of the control systems developed and to find optimal user defined parameters. The final simulations achieved both distance drift reduction and inter-satellite relative distance changes.

I. Nomenclature

a	=	semi-major axis, m
\bar{a}	=	mean semi-major axis, m
A_c	=	satellite cross-sectional area, m^2
a_D	=	acceleration due to atmospheric drag, m/s^2
a_r	=	relative acceleration, m/s^2
$c_{0,1,2}$	=	regression analysis coefficients
C_D	=	drag coefficient
d_r	=	relative distance, m
e	=	eccentricity, $^\circ$
ECI	=	Earth centered inertial frame
h	=	specific angular momentum, m^2/s
HD	=	high (maximum) drag orientation
i	=	inclination, $^\circ$
LD	=	low (minimum) drag orientation
m	=	satellite mass, kg
n	=	orbit multiplier for stabilization maneuver
p	=	orbit multiplier for regression analysis
q	=	number of data points
Q_{Xx}	=	orthogonal transformation matrix
R^2	=	coefficient of determination
R_e	=	radius of the Earth, m
r	=	radius magnitude, m
\bar{r}	=	radius vector, m
T	=	orbital period, s
\bar{T}	=	mean orbital period, s
t	=	time, s
t_D	=	maneuver delay duration, s
t_M	=	maneuver duration, s
v	=	free-stream velocity magnitude, m/s

*Graduate Research Assistant, Daniel Guggenheim School of Aerospace Engineering

\bar{v}	=	free-stream velocity vector, m/s
v_r	=	relative velocity, m/s
X	=	state space
x, y, z	=	ECI frame axis
Greek		
ϵ	=	allowable orbital period error, s
μ	=	standard gravitational parameter for Earth, $m^3 s^{-2}$
ρ	=	atmospheric density, kg/m^3
σ	=	allowable distance error, m
θ	=	true anomaly, $^\circ$
ψ	=	angular velocity, $rads/s$
$\dot{\psi}$	=	angular acceleration, $rads/s^2$
Ω	=	right angle of ascending node, $^\circ$
ω	=	angle of periapsis, $^\circ$
Subscripts		
$2B$	=	2 body dynamics
A	=	denotes Satellite A
AD	=	atmospheric drag
B	=	denotes Satellite B
i	=	increment
J_2	=	J_2 perturbation
X	=	in the ECI coordinate frame

II. Introduction

SMALL satellites continue to grow in importance in the aerospace community. The small, lightweight CubeSats can often be developed for a fraction of the cost of larger satellites. Because of this reduction in cost and complexity, and the increased ability to launch CubeSats easily, these spacecraft are being sent into orbit at an ever growing rate.

One challenge when dealing with small mass and size restrictions is that often satellites will forgo having any onboard propellant. For most of these satellites this trade off is worth it. The reduction in cost makes losing a spacecraft or orbital degradation more palatable, thus, there is less of a desire to prolong the satellite lifespan through propulsive maneuvers. Traditionally, most small satellite missions are also only for a single spacecraft, with no interaction or communication except with a ground station.

Where this becomes more complicated is that these CubeSats are now operating more often in clusters or constellations. Private companies can launch many small disposable satellites that can be easily replaced instead of large multi-billion satellites, which may have more capabilities, but also come with a much higher risk should the satellite fail or be damaged during launch.

With these new complex systems of satellites, new control theories and techniques are required to be developed. Since CubeSats often sacrifice propulsion in order to maximize the payload space, other methods of control must be used. The primary method that is being explored was proposed by Leonard, Hollister, and Bergmann in 1989, called differential drag[1]. This process is the concept where two satellites can alter their orientations, changing their drag profiles, and thus be able to have some control to maintain or reduce distances between satellites. It does require that the satellites are able to interact with some atmosphere, therefore, this concept is generally only used for spacecraft in low Earth orbit, LEO. When differential drag was proposed most satellites were still large and expensive, and if they operated in LEO the satellite lifespans would be extremely short. At that point in time this would be hardly ideal, so not much research was done in this area for the next couple of decades.

Over the last few years there has been much research into the study of differential drag on satellites. In 2004 Mishne looked at satellite control using drag variations and J_2 perturbations[2], while in 2011, in separate papers, Horsley and Kumar et al. both took more in depth looks at theoretical models for controlling multi-satellite formations using differential drag [3, 4]. Then, in 2013, Finley et al. looked at constellation phasing using differential drag for the CYGNSS satellites[5] and in 2014 Ben-Yaacov et al. evaluated stability and performance for a satellite cluster, also using differential drag[6].

During this same period, Planet (Formerly Planet Labs), a private company operating primarily out of San Francisco began deploying dozens of small satellites, all designed to work together in a large constellation. This has allowed them

to do real-world analysis, which they have published publicly[7, 8].

In 2012 Varma worked with Kumar to look at differential drag controller design for formation control[9], and then in 2014 Kumar et al. took a further dive into control law using atmospheric drag to maintain a formation[10]. Frey et al. also explored control theory, specifically for parameter governors of satellite formations[11]. A Lyapunov-based controller was researched by Perez and Bevilacqua in 2014[12], and in 2015 Anderson continued this work with the Air Force Research Lab, running simulations of the Lyapunov controller[13]. Perez and Bevilacqua also published a new paper in 2016, that followed and continued the research they were performing before[14]. In 2018 Di Mauro et al. looked at using continuous differential drag maneuvers for control of multiple spacecraft[15].

In 2008 Bevilacqua et al. published a paper on using differential drag for satellite rendezvous[16]. This was followed in 2014 to a paper by Harris et al. exploring minimum time for rendezvous[17] and in 2015 a paper by Dell’Elce et al. about optimal rendezvous[18].

There has also been work in understanding the various effects of error related to differential drag. In 2016 Ben-Yaacov looked at covariance analysis of cluster flight[19], while Mazal et al. published papers in 2015 and 2016 evaluating satellite rendezvous with uncertainties[20, 21].

With the usage of CubeSat constellations now at the forefront, differential drag research has had a resurgence. This paper will continue this research by developing two new types of automated formation control maneuvers for satellites that only use differential drag for control. This research is a continuation of the work performed by Groesbeck et al. for the Ranging and Nanosatellite Guidance Experiment (RANGE) satellites[22].

The RANGE CubeSats are two 1.5U ($1U = 10 \times 10 \times 10cm$) satellites that are identical in size and mass. These two satellites were designed to launch together, physically attached to each other. Once detumbling had been accomplished a small spring-loaded force would be applied to each satellite in opposite directions, causing the satellites to separate. They would then work in tandem, in a leader-follower formation, where they would perform experiments designed to improve the absolute and relative positioning capabilities of other small satellites. Due to the small size of the spacecraft and a mass limit of 2.5 kg, no onboard propellant was installed. Differential drag would be required to keep the satellites together and within the mission relative distance parameters to enable the science experiments to be performed. The RANGE satellites were launched in December of 2018, the data acquisition period overlapped with the development of the control systems in this paper. It is hopeful that these systems will be able to be used with the RANGE satellites to test their real-world performance. The work of this paper finished prior to the end of that period, so the systems designed in this paper were run through simulations only at the time of submission.

The work done in this paper will focus on two areas: the reduction of drift between satellites and changing the mean distance between two satellites. The drift reduction portion is important to keeping satellites a set distance apart within an allowable error tolerance. This is vital when satellites must keep a particular distance in order to meet the science objectives of a mission, such as the case for the RANGE satellites[23]. An issue with this particular mission is that the two satellites are launched together and separated by a small force, and while this force may be small, it can have drastic drift effects between the two satellites. The drift reduction system will be able to overcome this force and keep the satellites at a steady mean relative distance. This technique is different to prior research in that it will evaluate drift rate as a function of difference in orbital period. The satellites will operate in either a maximum drag, *HD*, or minimum drag, *LD*, orientation. This technique utilizes the two satellites working in tandem to create a steady mean distance between satellites with a minimum number of changes in orientation.

The second part of this paper focuses on the changing distance maneuvers. This system will allow the satellites to change the relative distance between them, enabling the satellites to either move closer together or further apart, depending on the needs of the mission. In the case of the RANGE satellites, the time it takes to overcome the initial force should leave the satellites beyond the allowable distance for the scientific mission. By bringing the two satellites closer together the mission parameters can be achieved. This system will be different from prior controllers. While it may not have some of the control that a Lyapunov or an LQR controller might have, by utilizing a phase-shift approach the satellites can achieve quicker changes in mean relative distance without the satellites making frequent, near constant, orientation changes. This method does require both satellites to maneuver in a coordinated method and they must be able to communicate with each other to enable better fidelity maneuvers, but this system allows the satellites to keep their nominal state in either the *HD* or *LD* orientation, and has the added benefit of performing autonomously without any need for human intervention. Other systems often work with a single driving satellite making changes in orientation. This can only be accomplished if the other satellite is in an orientation where the drag profile cannot be either maximum or minimum, as the driving satellite must be able to both speed up, slow down, and eventually match the velocity of the other satellite.

III. Drift Reduction

A. Theory

When dealing with a multi-satellite constellation, the spacing of those satellites can be vitally important. Often, satellites are deployed together, either physically fixed, or launched separately within a small time window. For either case, it is not uncommon for the satellites to have different orbital elements, even if they are minuscule differences. These small variations can cause satellites to drift apart or closer together, depending on their orbital period. If the drift is in the proper direction and magnitude this can be used to spread the satellites out to some distance. Once that relative distance has been achieved, the drift has to be removed so that the relative distance remains constant.

For the RANGE satellites another issue is present. These satellites launch together, physically attached. A small mechanism separates the satellites by imparting a small, instantaneous, force on each satellite in opposite directions. This small force behaves similarly to an instantaneous change in velocity and alters each satellite's orbital elements. This change is very minuscule, altering the semi-major axis, a , by only a few meters. But this change in a has the effect of creating a difference in orbital period, T . For the RANGE satellites, they may only have a difference in T of approximately 89.4 ms, but with a velocity at periapsis of 7.61 km/s this translates to a drift rate of 681 m every orbit. The mission parameters require that the satellites stay within certain distance bounds, which this drift rate would exceed before the science tests could be completed.

To overcome this drift factor a simple controller was designed. It should be noted that this system operates under the assumption that the satellites are in coplanar orbits and that the structure and masses are identical. The system is designed to work with two satellites, designated A and B , but can be used with any size constellation as long as any two satellites can be paired for this maneuver. The process for reducing the drift between two satellites can best be seen in the system diagram found in Fig. 1. In this diagram HD refers to the maximum drag orientation while LD refers to the minimum drag orientation.

In this diagram, the system begins with the initial state vectors. For the simulation, this was initially given in orbital elements and then converted to Cartesian coordinates in the Earth centered inertial, ECI, frame. From these values, a for each satellite was computed using Eq. 1[24, 25].

$$a_{A,B}(t) = \frac{1}{\frac{2}{r(t)} - \frac{v(t)^2}{\mu}} \quad (1)$$

It is important to use this semi-major equation for an elliptical orbit because a simplified, circular, orbit equation will reduce the fidelity of the system and cause failures in the simulation. This equation can then be inserted into Eq. 2 to compute the initial orbital period, T , for each satellite.

$$T_{A,B}(t) = \sqrt{\frac{a(t)^3}{\mu}} \quad (2)$$

At this point, the system enters the closed-loop control that will keep the satellites from drifting apart. The first step is that system will evaluate the relationship between the two satellites' orbital periods. This assumes that the satellites will have some form of inter-satellite communication such that they know their position in relation to each other. If the orbital period for satellite A , T_A , minus the orbital period for satellite B , T_B , is greater than an allowable error, ϵ , then A will go into the HD orientation while B will enter an LD orientation.

This is because a satellite that has a higher orbital period will take longer to circumnavigate the globe than the other satellite. This difference is what is causing the orbital drift. To overcome this, the satellite with the higher orbital period will decrease its altitude, which is accomplished by increasing its drag profile relative to the other satellite. That is why when the inverse is true, $T_B - T_A \geq \epsilon$, A will go into an LD orientation and B will go into an HD orientation.

If neither case is true, then the satellites are within the allowable error for their drift. In this case both A and B will enter their HD orientation. It should be noted, that for this scenario, there is an understanding that both satellites will have the same HD profile and drag coefficients. If their HD profiles are not the same then the satellites will have a relative distance drift rate. This case also uses the HD orientation as the default position because it allows the RANGE satellites to have their antennae pointed towards Earth, which helps with the satellite communication. This orientation does decrease the lifespan of the satellites, though, so for other cases the LD orientation may be preferable.

For the simulation, the satellites are then propagated forward in time using an ODE45 propagator with a time increment of t_i . For a satellite that is actually in orbit, this stage would be substituted by receiving data from either GPS satellites or a ground station. From this data, a new a and T for each satellite is computed. The next step is a test to

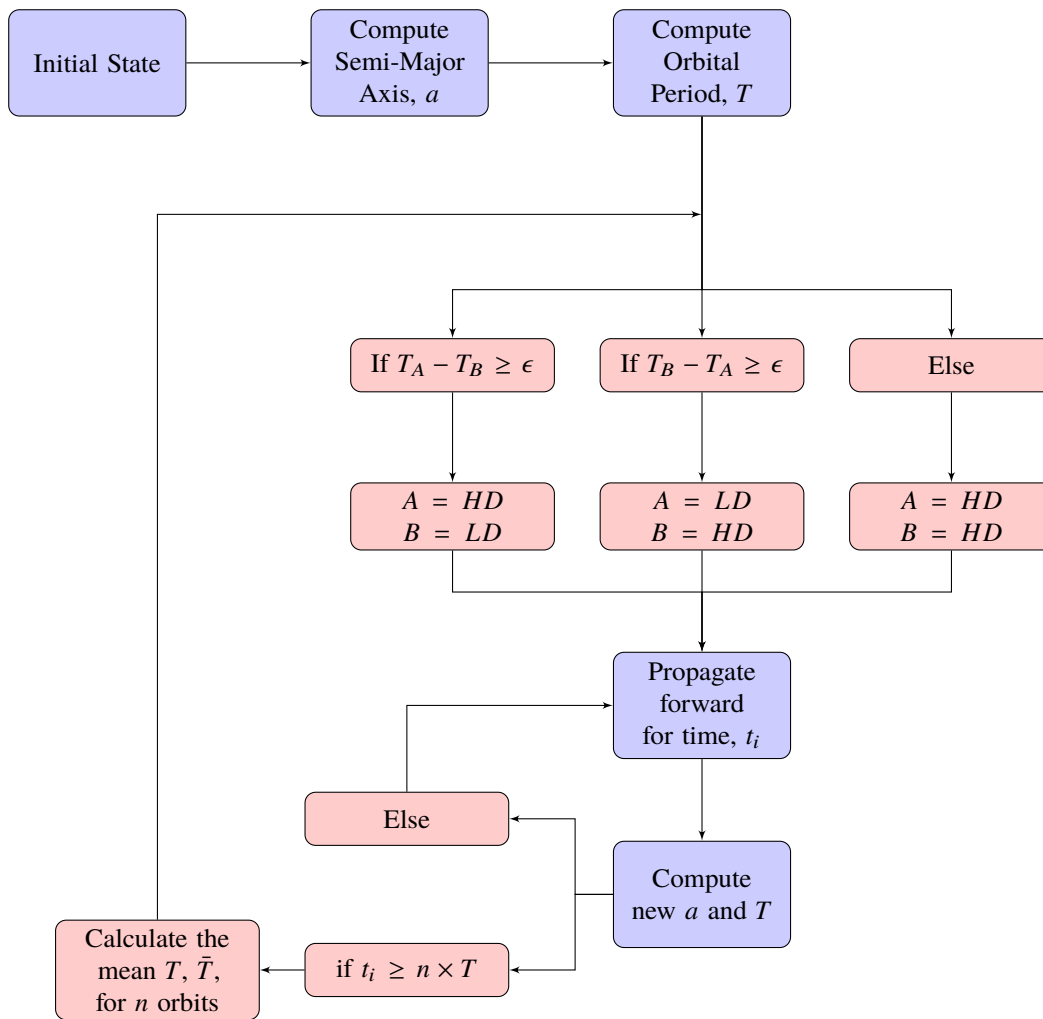


Fig. 1 Drift Reduction System

evaluate if enough time has passed to enable the drift analysis to be performed. This is done by checking to see if t_i is greater than a user chosen constant, n , multiplied by the latest T . If this value has not been achieved then the system loops back on itself, continuing the propagation. If the value has been exceeded then the system will take the mean orbital period, \bar{T} , over the last n orbits. This value is a rolling value, always evaluating over the latest n orbits. Since T can fluctuate in a similar fashion to a sine wave, this makes sure that \bar{T} is evaluated over a set frequency. When \bar{T} has been computed, the system then loops back to before the T evaluation and runs through the comparison and evaluation again, altering the orientations as required to achieve a steady mean distance between the satellites.

B. Simulation Results

A simulation was performed using MATLAB and an ODE45 propagator. The initial conditions were an inclination, i , of 90° , an eccentricity, e , of 1×10^{-12} , an altitude of 450 km , and the right angle of ascending node, Ω , argument of periapsis, ω , and true anomaly, θ , all set to 0° . A 2 cm instantaneous change in velocity was imparted on both satellites in opposite directions along the direction of travel. The satellites' mass, m was set to 2.5 kg . The scenario was run for 5 days at 15 second time increments. For the orbital dynamics, 2-body gravity effects, Eq. 3, were used along with J_2 perturbations, Eq. 4. For these equations, $\mathbf{0}$ denotes an empty quadrant; the state spaces (x, y, z) are in the inertial frame; r denotes the radius magnitude; and μ is the standard gravitational parameter for Earth, $3.986 \times 10^{14} \text{ m}^3 \text{ s}^{-2}$. The J_2 constant is 1082.64×10^{-6} and R_e denotes the radius of the Earth, $6.37815 \times 10^6 \text{ m}$.

$$\dot{X}_{2B} = \begin{bmatrix} \dot{x} \\ \dot{y} \\ \dot{z} \\ \ddot{x} \\ \ddot{y} \\ \ddot{z} \end{bmatrix} = \begin{bmatrix} & & & 1 & 0 & 0 \\ & \mathbf{0} & & 0 & 1 & 0 \\ & & & 0 & 0 & 1 \\ -\frac{\mu}{r^3} & 0 & & & & \\ 0 & -\frac{\mu}{r^3} & & & \mathbf{0} & \\ 0 & 0 & -\frac{\mu}{r^3} & & & \end{bmatrix} \begin{bmatrix} x \\ y \\ z \\ \dot{x} \\ \dot{y} \\ \dot{z} \end{bmatrix} \quad (3)$$

$$\dot{X}_{J2} = \begin{bmatrix} \dot{x} \\ \dot{y} \\ \dot{z} \\ \ddot{x} \\ \ddot{y} \\ \ddot{z} \end{bmatrix} = \frac{3}{2} J_2 \mu \frac{R_e^2}{r^4} \begin{bmatrix} & & & \mathbf{0} & & \mathbf{0} \\ & & & 0 & & 0 \\ \frac{1}{r} (5 \frac{z^2}{r^2} - 1) & 0 & & 0 & & \\ 0 & \frac{1}{r} (5 \frac{z^2}{r^2} - 1) & & 0 & & \mathbf{0} \\ 0 & 0 & & \frac{1}{r} (5 \frac{z^2}{r^2} - 3) & & \end{bmatrix} \begin{bmatrix} x \\ y \\ z \\ \dot{x} \\ \dot{y} \\ \dot{z} \end{bmatrix} \quad (4)$$

For the differential drag component a simplified atmospheric force model was used. The system uses a constant atmospheric density, ρ , of $1.28 \times 10^{-12} \text{ kg/m}^3$. The satellites are assumed to be in either the *HD* orientation with a cross-sectional area, A_c , of 0.0045 m^2 and a drag coefficient, C_D of 2.5064, or a *LD* orientation with an A_c of 0.01 m^2 and a C_D of 3.7516. These values were based off previous research performed by Hart et al. for the RANGE satellites[26]. The atmospheric drag, a_D , was then computed using Eq. 5, where \bar{v} is the free-stream velocity vector. This value was then used with Eq. 6 to get the values for in inertial frame.

$$a_D = -\frac{1}{2} \frac{C_D A_c \rho v^2}{m} \quad (5)$$

$$\dot{X}_{AD} = a_D \frac{\bar{v}}{v} \quad (6)$$

These three dynamics equations were then combined in Eq. 7 to give the dynamics for the entire system in state space form.

$$\dot{X} = \dot{X}_{2B} + \dot{X}_{J2} + \dot{X}_{AD} \quad (7)$$

To better understand what the allowable error, ϵ and the orbital period multiples, n , should be, 12 different scenarios were run. The first four were run with an ϵ of 0.0001 s . These four used an n of 0.5, 1, 2, and 3, respectively. Figure 2 is the results from these first four runs. This process was then repeated for $\epsilon = 0.0010 \text{ s}$ and $\epsilon = 0.01 \text{ s}$ and for each of

the same previous n . These results are in Figs. 3-4. For each plot, the orientation of each satellite is also shown. The satellites operate on a binary method, either in the HD or LD orientations. For the plots, when "A HD" is non-zero, it is considered to be in the maximum drag orientation. This is the same case for "B HD". When either plot is at zero they are considered to be in the minimum drag orientation. The y-axis magnitude of the orientation plots has no bearing and are only used to help with visualization.

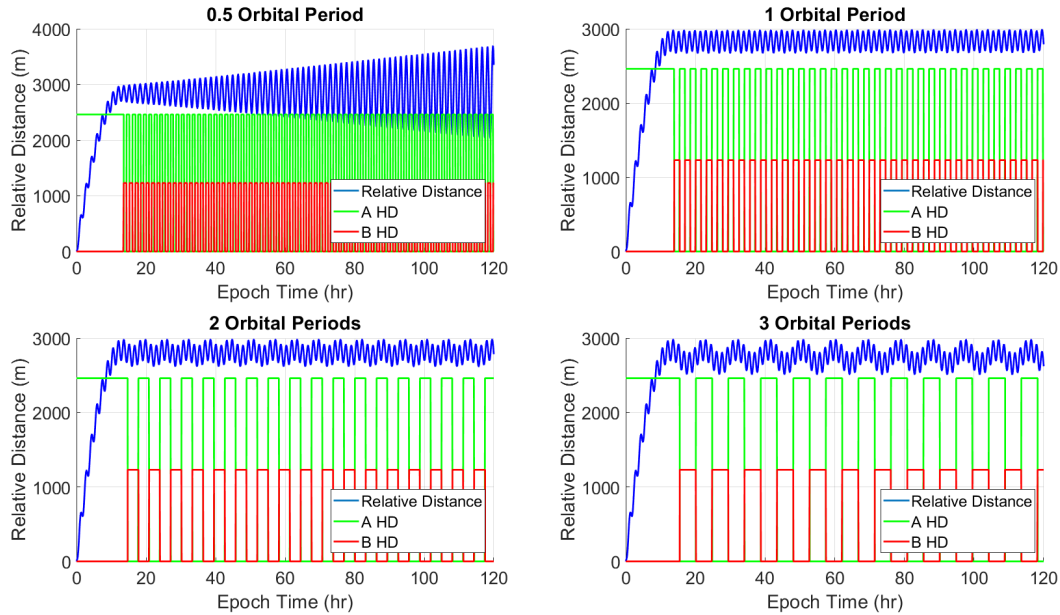


Fig. 2 Evaluation of Drift Reduction Maneuver with $\epsilon = 0.0001 s$

For the ϵ of 0.0001 s , it can be observed that for all four values of n a steady mean distance is achieved. For the 0.5 orbital period, while the mean relative distance remains steady, the magnitude of the oscillations grows. This is in part because the satellites are changing orientations at a rapid pace, swapping orientations nearly twice per orbit. This maneuver schedule keeps the semi-major axis for both satellites close together, but adds a small amount of eccentricity with each orbit. There is also a 180° angle between the two satellites' periapsis, so as this eccentricity grows, the distance between one satellite's periapsis and the other satellite's apoapsis also increases, leading to the growth of the frequency's magnitude.

The 1 orbital period scenario overcomes the drift, reaching a mean steady distance of 2828 m , in approximately 14 hours. The time when this occurs will be referred to as the critical point, as this point is the same for all values of n and ϵ . The 2 and 3 orbital periods also keep the same mean steady distance, but a secondary oscillation is added. This is in part because the mean distance evaluation is performed for longer periods and the satellites perform changes in orientation less often to compensate for any residual drift. It should also be noted, that at the scenario altitude, the speed of the satellites is 7.641 km/s , therefore a difference in orbital periods of 0.0001 s would result in a possible residual drift of 0.7641 m per orbit, or less than 15 m per day of potential drift.

When ϵ was raised to 0.0010 s similar results were observed, Fig. 3. In this case, the 0.5 orbital period still reaches the critical point, but the mean distance calculations are done in such a way as to not see the satellite drift adequately. For the other three cases there is very little noticeable difference in the relative distance plots from the previous ϵ plots. Where there is a difference is in the frequency of changes in satellite orientations. In the previous case, both satellites changed their orientations at the same time, meaning that the satellites were always in opposite orientations. The challenge with this is that if the satellites needed to be in the HD orientation to communicate with the ground station, only one satellite would be able to communicate at a time. With the higher ϵ , the amount of time spent in LD is decreased and there are small windows where each satellite is spent in the HD mode. This both lengthens the communication window and allows for both satellites to communicate with the ground station at the same time. Also of note, with the same satellite speed as before but with the increase in ϵ , there is a potential maximum drift of 7.641 m per orbit or about 138 m per day.

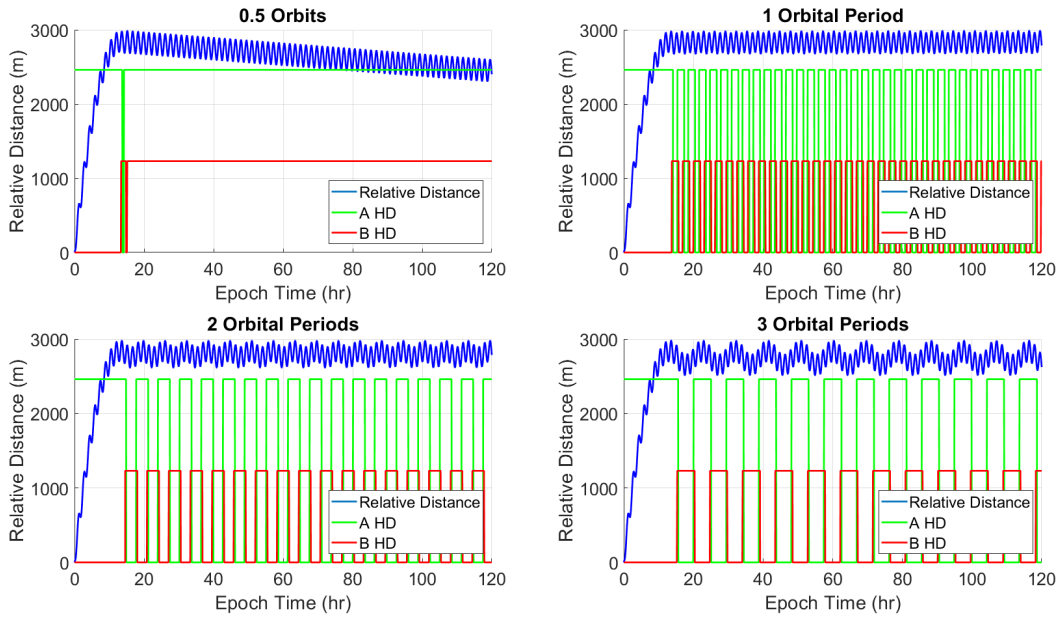


Fig. 3 Evaluation of Drift Reduction Maneuver with $\epsilon = 0.0010$ s

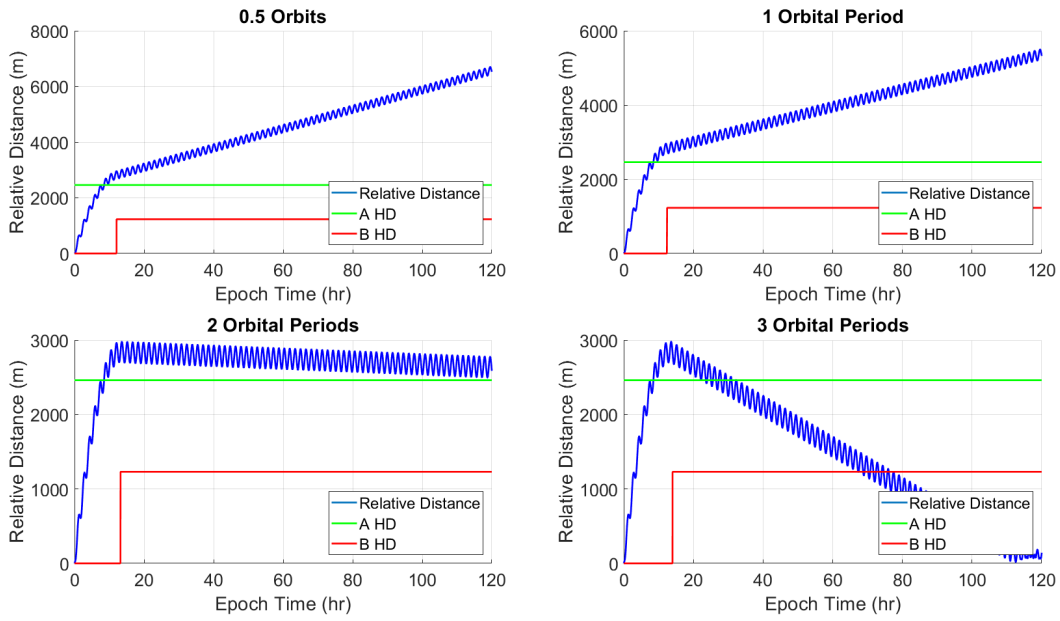


Fig. 4 Evaluation of Drift Reduction Maneuver with $\epsilon = 0.0100$ s

For the final four evaluations, where ϵ was raised to 0.0100 s , Fig. 4, there is a large difference in results. All four cases still reach the critical point, but the allowable drift error is large enough that the satellites never reach a steady mean distance. Depending on very small differences in when the critical point is reached, the satellites can either drift towards or away from each other. With the 7.641 km/s speed, 0.0100 s error equates to a possible 76.41 m per orbit drift, or 1.375 km per day. This error is therefore too large to be acceptable for the mission parameters that would be most likely needed for formation flying. Additionally, scenarios were run for each orbit with an ϵ of 0.1000 s , but for all cases the critical point was never reached, as the allowable drift exceeded any drift caused by the separating force.

Depending on the criteria of the mission goals and the hardware restrictions of the satellites, the operators could choose 1, 2, or 3 orbits with an allowable error less than 0.0100 s . The drivers would be the trade off of having to have more changes in orientation versus adding a secondary oscillation to the mean distance. For the RANGE satellites, it was deemed that having a finer mean steady distance would be more valuable, so further studies of allowable error were performed for the 1 mean orbital period scenario.

In Fig. 5, the results of six different ϵ values are displayed. The values plotted are for ϵ of 0.0001 s and 0.0010 s , which were done before, along with a midpoint between the two, 0.0005 s , and increases of 0.0010 s until ϵ reaches 0.0040 s .

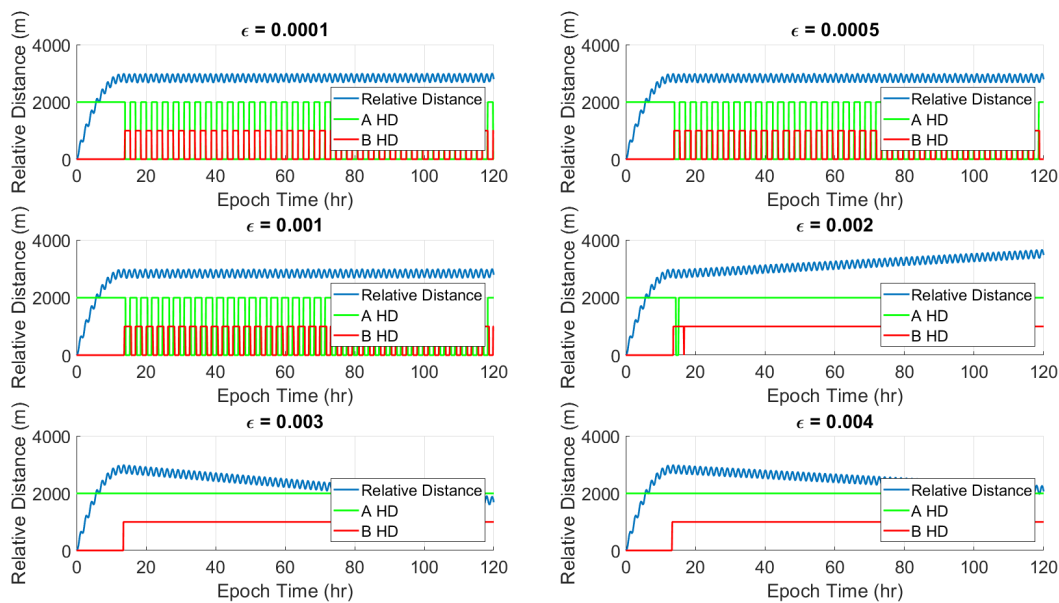


Fig. 5 1 Mean Orbital Period with Variable Error Evaluation

From this study it is seen that when ϵ is 0.0020 s a second small corrective maneuver is done to overcome an initial drift, but the residual drift that is left over allows the satellites to not maintain a steady mean relative distance. For the cases of ϵ equaling 0.0030 s and 0.0040 s , the critical point is reached, but the residual drift is large enough to not allow the satellites to reach a steady distance as well. If finer refinement is required, further studies could be done between 0.0010 and 0.0020 s , but for the RANGE mission it is believed that an n of 1 and an ϵ of 0.001 s should be sufficient. These values would keep the satellites at a steady mean distance, reduce any secondary oscillations, and would minimize the number of changes in orientation while allowing for some windows where both satellites are in the *HD* orientation at the same time.

IV. Distance Maneuvers

A. System Design

The second automated control relates to satellites where there is a wish to change the relative distance between them. This series of maneuvers can be important for rearranging satellites within a constellation, or in the case of the RANGE

satellites, for placing the satellites at specific distance to perform scientific tests. As shown in the preceding section, when overcoming a separation force to achieve a steady mean distance, the final distance between satellites may be greater than the mission parameters allow. In the previous case, the satellites end up nearly 3000 meters apart, and if the required distance were no more than 1000 meters, the satellites would need to reduce that distance by at least 2000 *m*.

The basis for the maneuvers was previously derived in Groesbeck et al.[22]. That paper displays that for two satellites using propellantless propulsion, if the satellites wish to change the relative distance, d_r , between them then a combination of maneuvers must be performed by both satellites. This desired change in distance, Δd_r can be achieved by just one satellite, but only if the other satellite is in an orientation that does not place it in either the maximum or minimum drag profile. For a scenario such as the RANGE satellites, where the default position is in the *HD* orientation, if only one satellite performs a maneuver there will always be a residual drift factor left over. The second satellite's maneuvers counteracts this drift by performing the same maneuver for the same amount of time, t_M , just at a delayed period, t_D , later. This allows the two satellites to start at the same altitude and to finish at the same altitude when the maneuvers are done, thus reducing any imparted drift.

For the satellites to perform these maneuvers both t_M and t_D must be computed. To do this, only two other variables are required; the relative acceleration rate between them based on a change in orientation, a_r , and the desired change in distance, Δd_r . Eq.'s 8 and 9, were derived in the previous paper and are what the satellites will use to calculate their maneuver schedule.

$$t_M = \sqrt{\frac{2\Delta d_r}{a_r}} \quad (8)$$

$$t_D = \frac{\Delta d_r}{a_r t_M} = \sqrt{\frac{\Delta d_r}{2a_r}} \quad (9)$$

The desired change in distance is something that would initially be provided by the user, in this case, the ground station. This could be a scenario where maybe the two satellites are five thousand meters apart, but a science objective may need the satellites to be within two thousand meters. In this case, the Δd_r would be -3000 *m*. The other value needed, a_r , is harder to get. In an ideal scenario this would be known beforehand, but because of the incomplete knowledge of atmospheric effects on drag and possible unknown prediction of solar flux, only a best estimate can be provided prior to launch. A better solution would be for the satellites to be able to compute their relative acceleration rate as they are performing the maneuver. For this paper, the solution to this problem is done through a 2nd order polynomial regression analysis.

The full system control that was developed can be found in Fig. 6. For this scenario, since an ODE45 propagator was used in MATLAB, all satellites start with an initial state. For simplicity, the trailing satellite will always be designated as satellite A. Just as for the drift reduction system, the semi-major axis, a , at that time is computed along with the orbital period, T , for each satellite. The system is then given a command of a Δd and depending on whether that distance is positive or negative, one of the satellites will enter the *LD* orientation. This operates under the assumption that both satellites are starting from the default *HD* orientation.

Once this has happened, the system propagates both satellites forward for a time increment of t_i . It then computes a new a and T value for each satellite. Since the relative distance is what is desired the system converts the ECI location data to the relative frame using the Clohessy-Wiltshire equations[25]. To compute the relative values, the first step is to find the specific angular momentum, h , of the chief satellite using Eq. 10, here designated as satellite A.

$$\bar{h}_A = \bar{r}_A \times \bar{v}_A \quad (10)$$

The next step is to compute the orthogonal transformation matrix, Q_{Xx} , using Equation 11. Additionally, the angular velocity, ψ , and angular acceleration, $\dot{\psi}$, can be calculated using Eq.'s 12-13.

$$Q_{Xx} = \begin{bmatrix} \frac{\bar{r}_A}{r_A} \\ \frac{\bar{h}_A \times \bar{r}_A}{h_A r_A} \\ \frac{\bar{h}_A}{h_A} \end{bmatrix} \quad (11)$$

$$\psi = \frac{\bar{h}_A}{r_A^2} \quad (12)$$

$$\dot{\psi} = -2 \frac{\bar{v}_A \cdot \bar{r}_A}{r_A^2} \psi \quad (13)$$

These can then be used with Equation 14 to find the relative distance, d_r , velocity, v_r , and acceleration, a_r ; Eq.'s 15-17. The final step is to then have the relative values rotated into the proper frame using the orthogonal transformation matrix multiplied by the relative values. Eq. 18 is an example of the process that is done for each relative motion value. The extra subscript, X , denotes if it is in the Cartesian frame.

$$\bar{a}_A = -\mu \frac{\bar{r}_A}{r_A} \quad (14)$$

$$\bar{d}_{r,X} = \bar{r}_B - \bar{r}_A \quad (15)$$

$$\bar{v}_{r,X} = \bar{v}_B - \bar{v}_A - \psi \bar{d}_{r,X} \quad (16)$$

$$\bar{a}_{r,X} = \bar{a}_B - \bar{a}_A - \dot{\psi} \bar{d}_{r,X} - \psi(\dot{\psi} \bar{d}_{r,X}) - 2\dot{\psi} \bar{v}_{r,X} \quad (17)$$

$$\bar{d}_r = [Q_{Xx}] \bar{d}_{r,X} \quad (18)$$

The values for v_r and a_r that are computed here are stored in the simulation for verification purposes only and are not used within the control system. The relative dynamic computation step would not be required for an onboard satellite cpu, but is included here to help with visualization and verification purposes. Likewise, since the assumption is made that the satellites are coplanar and the along-track relative distance is much larger than the radial relative distance, the magnitude of the vector can be taken and assumed as the distance between the satellites.

The system then does a check to see if the elapsed time has met a predefined moment, which will be a user chosen constant, p , that is multiplied by the orbital period. This value is discussed further in Section IV.B. If this time check has not been passed then the system loops back and continues its propagation until this condition has been met. Once this has occurred, a second order regression analysis is done of the relative distance since the change in distance command was given. The second derivative of that equation is then taken and a final a_r is obtained. Now that this value is known, a t_M and t_D can be computed.

The system then enters the command phase. Based upon what the computed t_M and t_D are, and depending on whether the maneuver is reducing or increasing the distance, $\pm \Delta d$, the system will change the satellites' orientations accordingly. These new orientations are then fed back into the propagator and the satellites are moved forward in time until the maneuvers are completed.

B. Regression Analysis

To test the regression analysis the following satellite parameters were used: inclination, $i = 90^\circ$, eccentricity, $e = 1 \times 10^{12}$, an altitude of 450 km, right angle of ascending node, Ω , and angle of periapsis, ω , of 0° . Satellite A has a true anomaly, θ_A of 0° , while Satellite B has θ_B of 0.042° , which translate to a starting mean relative distance of 5000m. To test the system the satellites' initial states are designed to be optimal, with no oscillatory behavior between them.

From Groesbeck et al.[22] it is understood that the satellites relative distance when in different, but constant, orientations will follow very close to a 2nd order polynomial, such as seen in Eq. 19.

$$d_r = c_0 + c_1 t + c_2 t^2 \quad (19)$$

This can be rewritten as a linear algebraic expression as Eq. 20, where q is the total number of data points being evaluated. These data points are all the values from t_0 to t_i or d_{r_0} to d_{r_i} . To solve for the polynomial coefficients, $c_{1,2,3}$ the linear expression is rewritten as Eq. 21.

$$\begin{bmatrix} q & \sum(t_i) & \sum(t_i^2) \\ \sum(t_i) & \sum(t_i^2) & \sum(t_i^3) \\ \sum(t_i^2) & \sum(t_i^3) & \sum(t_i^4) \end{bmatrix} \cdot \begin{bmatrix} c_0 \\ c_1 \\ c_2 \end{bmatrix} = \begin{bmatrix} \sum(d_{r_i}) \\ \sum(t_i \cdot d_{r_i}) \\ \sum(t_i^2 \cdot d_{r_i}) \end{bmatrix} \quad (20)$$

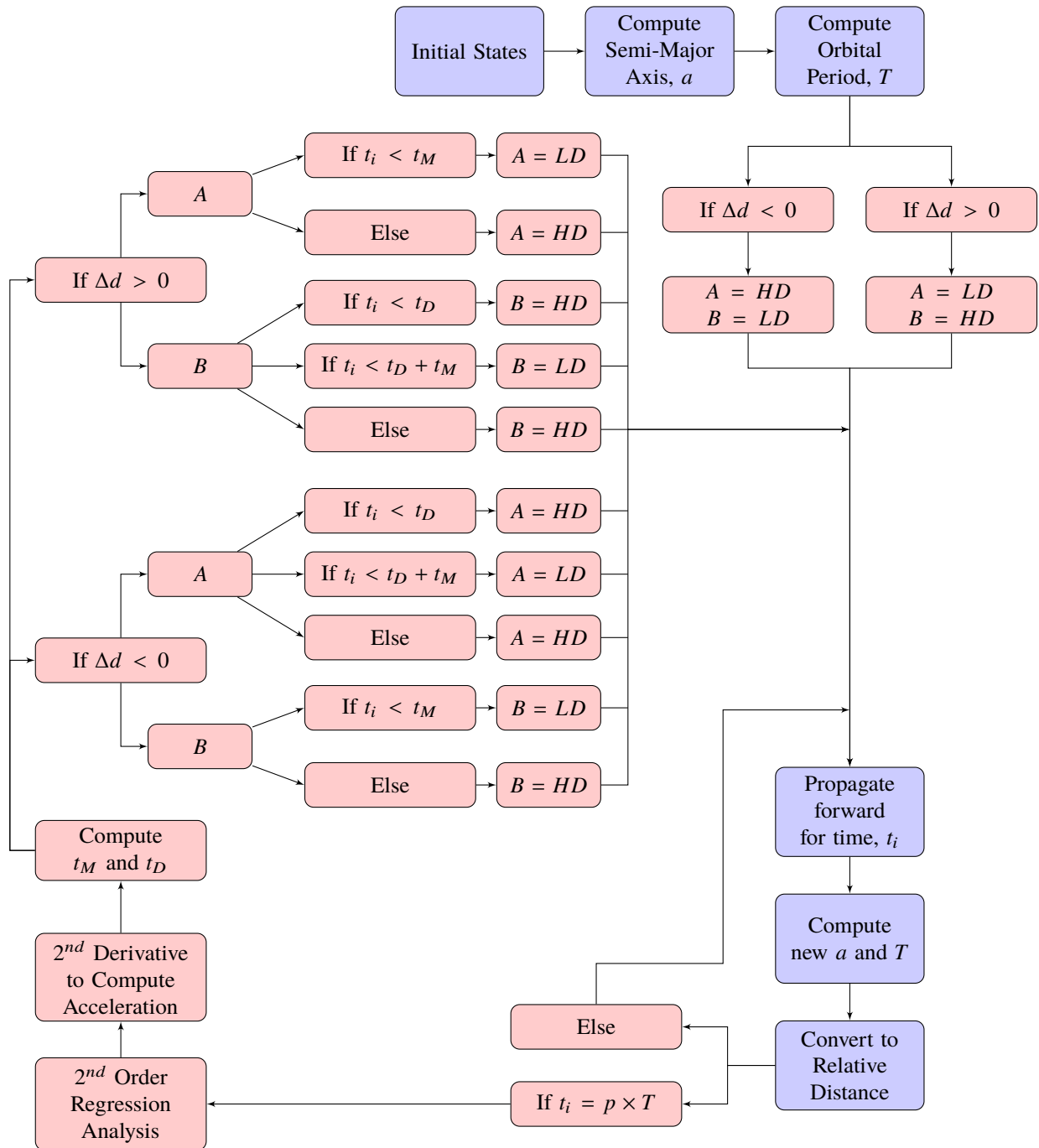


Fig. 6 Distance Maneuver System

$$\begin{bmatrix} c_0 \\ c_1 \\ c_2 \end{bmatrix} = \begin{bmatrix} q & \sum(t_i) & \sum(t_i^2) \\ \sum(t_i) & \sum(t_i^2) & \sum(t_i^3) \\ \sum(t_i^2) & \sum(t_i^3) & \sum(t_i^4) \end{bmatrix}^{-1} \cdot \begin{bmatrix} \sum(d_{r_i}) \\ \sum(t_i \cdot d_{r_i}) \\ \sum(t_i^2 \cdot d_{r_i}) \end{bmatrix} \quad (21)$$

The final step is to solve for the relative acceleration. This is done by taking the second derivative of Eq. 19, which results in Eq. 22.

$$a_r = 2c_2 \quad (22)$$

To find an optimal user inputted orbital period multiplier, p , which will determine the amount of time required for a satisfactory relative acceleration rate, a regression analysis was done where two satellites entered opposite orientations and stayed in that mode. Satellite A was placed in the *LD* orientation while B was placed in the *HD* orientation. The relative acceleration was computed continuously, with each time increment adding a data point to the analysis. Figure 7 shows the changing relative distance as a function of time and Fig. 8 is the computed relative acceleration as a function of increased data points, reflected as time.

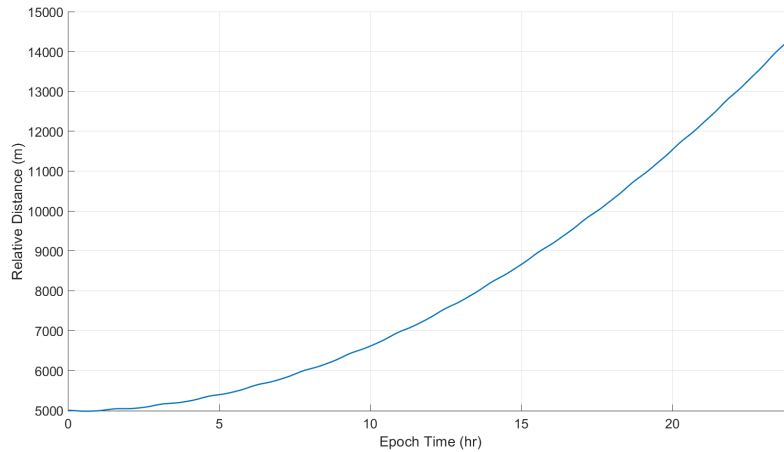


Fig. 7 Relative Distance as a Function of Time with the Satellites Moving Away from Each Other

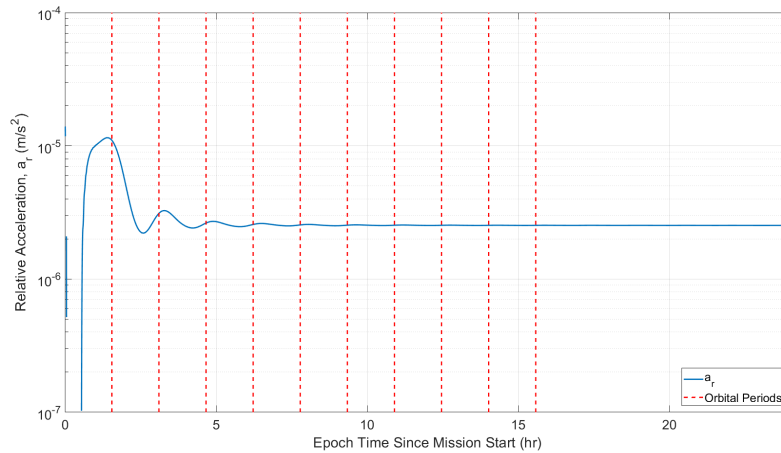


Fig. 8 2nd Order Regression Analysis of Acceleration as a Function of Time

To understand how well the analysis was performed the coefficient of determination, R^2 was computed. This was done for each increase in data points, so just as before the data points range from t_0 to t_i and d_{r_0} to d_{r_i} . Additionally, the value \bar{d}_{r_i} is the mean over that range. Eq. 23 was used to compute the R^2 values while Fig. 9 is the R^2 of that analysis as a function of increased data points, also represented as epoch time.

$$R^2 = \frac{\sum(d_{r_i} - \bar{d}_{r_i})^2 - \sum(d_{r_i} - c_0 - c_1t_i - c_2t_i^2)^2}{\sum(d_{r_i} - \bar{d}_{r_i})^2} \quad (23)$$

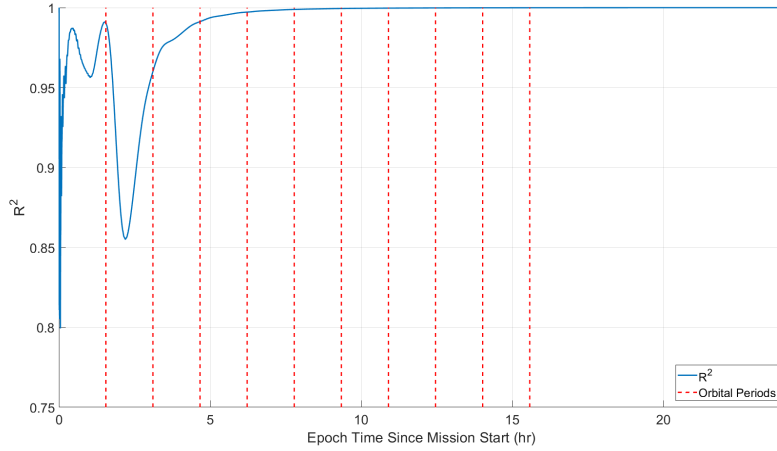


Fig. 9 2nd Order Regression Analysis of R^2 as a Function of Time

From these plots, a convergence value of $a_r = 2.5307 \times 10^{-6} m/s^2$ was found. The R^2 stays consistently high throughout, but approaches 1 by the fifth orbit. Since this is a significant amount of time, the third orbit was chosen as the p multiplier, since at this point R^2 is at 99.13% and the relative acceleration value at this point is $2.6331 \times 10^{-6} m/s^2$ which gives a percent error of 3.89%.

A similar process was then done to see if there was any difference in relative acceleration when the satellites begin to approach each other. For this scenario, satellite A was placed in the *HD* orientation and B was placed in the *LD* orientation. Figures 10-12 are the same series of plots that were performed before, though the a_r plot had to be displayed in a traditional format instead of the log axis because the values move regularly from positive to negative until the values begin to converge.

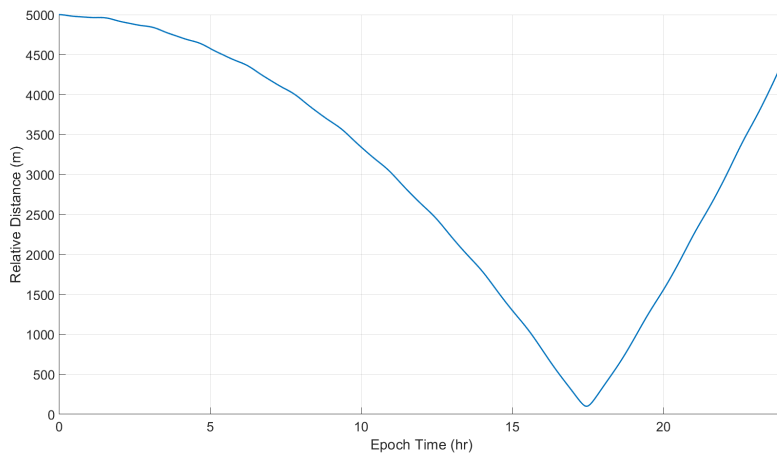


Fig. 10 Relative Distance as a Function of Time with the Satellites Moving Towards from Each Other

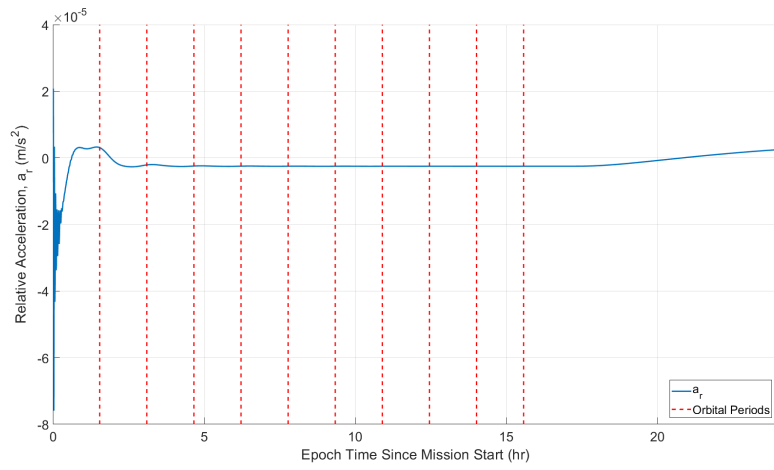


Fig. 11 2nd Order Regression Analysis of Acceleration as a Function of Time

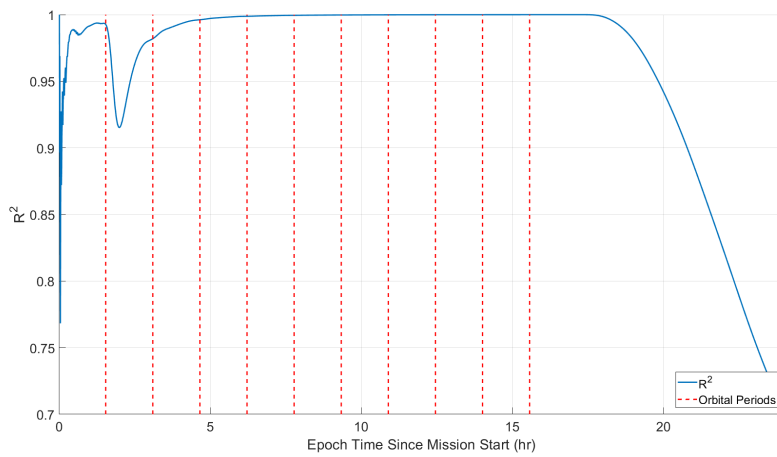


Fig. 12 2nd Order Regression Analysis of R^2 as a Function of Time

The biggest difference for this scenario is that given enough time the satellites over take each other. This required that the relative acceleration convergence point be evaluated before this happens. From the data, a_r was found to be $-2.5205 \times 10^{-6} m/s^2$, which is nearly identical to the other test, though in the negative direction. Similarly, the R^2 value approaches 1 until the satellites exchange positions and the R^2 begins to drastically fall. The third orbit appears to be a valid p value as this achieves an a_r of $-2.4544 \times 10^{-6} m/s^2$ which is a percent error of 2.694% and the R^2 is 99.62%.

The final test was to look at a less ideal orbit. As seen from drift reduction maneuver simulation in III.B, the two satellites could easily have a more oscillatory mean relative distance. A scenario was run where the radius and velocity vectors in the ECI frame from the end of the previous simulation were used. The satellites then performed the same operation as for the first test, where satellite A and B are in an *LD* and *HD* orientation, respectively. Figures 13-15 are the results.

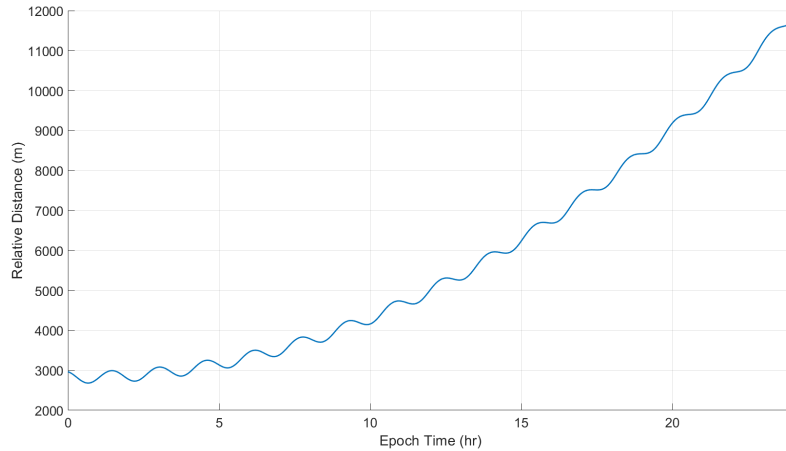


Fig. 13 Relative Distance as a Function of Time with the Satellites Moving Away from Each Other and Oscillating

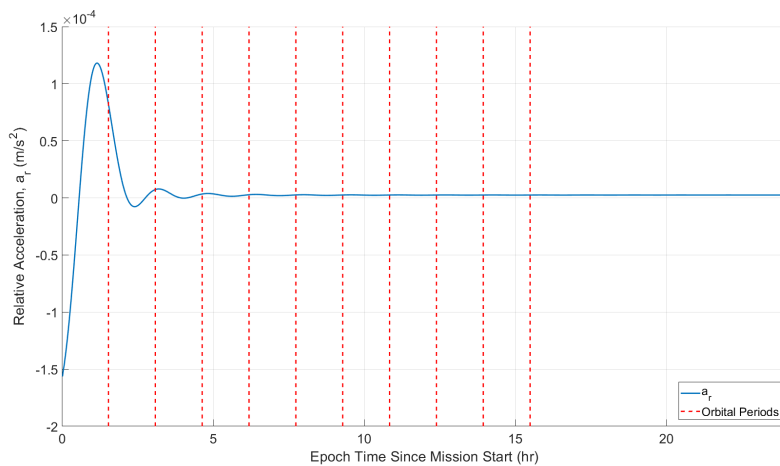


Fig. 14 2nd Order Regression Analysis of Acceleration as a Function of Time

From the relative distance plot it is easy to see that the same pattern of growth happens, but that the oscillatory nature adds complexity that will complicate the regression calculations. From the a_r plot the values still converges with a final result of $2.5288 \times 10^{-6} m/s^2$, which is still nearly identical in magnitude to the previous cases. In the R^2 plot we can see that it stays relatively close to 1 for less than one orbit before dropping to below 10%. While it does begin to climb, it takes over 5 orbits before it is above 90%. By the third orbit this value is $3.4528 \times 10^{-6} m/s^2$, with an R^2 of

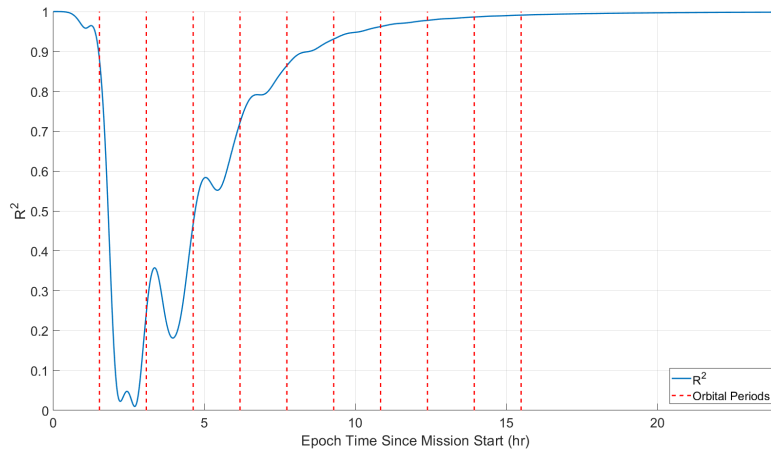


Fig. 15 2nd Order Regression Analysis of R^2 as a Function of Time

47.57% which corresponds to a percent error of 26.68%. This variation leads to errors that will be talked about in the next section.

C. Initial System Results

To test the maneuver system, the non-oscillatory scenario, used first in Section IV.B, was used. The satellites were given a command to move 3000 meters further apart in relative distance. The regression test was performed for 3 orbital periods before the computation of t_M and t_D was performed. The results of this procedure can be seen in Fig. 16.

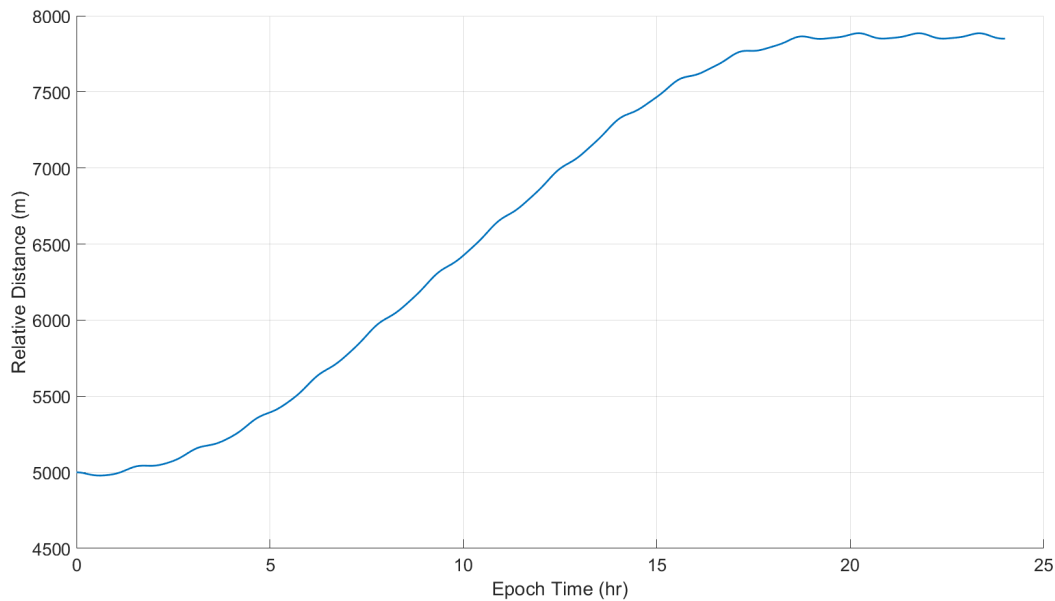


Fig. 16 3000 Meter Distance Maneuver with Original System (may need to change this)

From this test it can be observed that the satellites do change their relative distance to each other and the final distance remains steady. Unfortunately the final distance is slightly undershot, at 2866 meters changed. This is a percent error of 4.693%. This error is due to the relative acceleration computation. At the point of 3 orbits, a_r was computed to be $2.633 \times 10^{-6} m/s^2$. This led to a value of 47,736 s, or 13.26 hr, for t_M and a value of 23,868 s, or 6.63 hr, for t_D .

A second potential problem with this maneuver schedule was also found. Even if it is assumed that the convergence value of a_r could be found within 3 orbits, with an orbital period of 93.19 minutes, the minimum distance for a change in distance maneuver is 1482 meters. This is because any less distance would compute a delay in maneuver time, t_D , that happens before the three orbital period evaluations are over, thus missing the point when the second satellite is supposed to begin its change in orientation. If this command is issued too late, the satellites end up out of sync and not only will the final distance be missed, but the satellites will have an inherent drift rate.

D. System Design Modifications

To solve the problems discovered in the first simulation results, two areas are focused on; situations where the change in distance is small leading to the system not having enough time to do a proper regression analysis, and overcoming the final distance error due to the error in the relative acceleration value from the regression. These are discussed further below and the final modified system can be found in Fig. 17.

1. Regression Analysis Modification

The minimum distance issue was solved by adding a small bypass to the controller. This bypass is marked in Fig. 17 with red text and arrows. This bypass computes what t_M and t_D would be if it was supplied a predetermined a_r . For this simulation the convergence value found before, $a_r = 2.5307 \times 10^{-6} m/s^2$, was used. If this were a real scenario and not a simulation, it would be recommended to let the satellites drift apart for 9 or more orbits and to calculate an a_r value that best matches the true satellite dynamics. Alternatively, as long as the first maneuver exceeds the minimum distance mentioned before, the calculated a_r for that initial maneuver could be stored as the default a_r until another maneuver is performed that exceeds the minimum distance.

With a t_M and t_D calculated, a check would be done to see if either of those values were less than the multiplier, p , times the orbital period. If that is true, then the regression analysis steps will be skipped and those maneuver times will be used instead. If this is not the case, then the system continues on as it was regularly designed, calculating an a_r based off of the regression analysis.

2. Final Distance Modification

To overcome the change in distance error, a slight modification to the system was added. This modification is marked with blue text and arrows in Fig. 17. The solution was to create a second closed-loop evaluation of the system. Once the entirety of the first maneuver is completed, the system evaluates the mean distance the satellites are at. At least one orbit is required to get this data, which is what this simulation used. For higher fidelity this evaluation could be done over more orbits, as long as they are done in orbital period increments.

The system then checks the desired final distance minus the evaluated final distance to see if it is less than a user defined distance error, σ . For this simulation, σ was chosen to be 10 meters, but depending on the user requirements, this value could be set as either a number or a percent error of the change distance. If the distance is greater than σ then the system computes a new desired change in distance, Δd , that would target the original distance. Once this loop has satisfied the σ error limit the simulation will end.

E. Modified System Results

The same scenario that was initially run was run again, but this time with the modified system. Fig. 18 is the result of this test.

It can be observed that after the first maneuver the system evaluated the distance error and made a second corrective maneuver to reach the final goal. This maneuver also only needed to be a positive 134 meters, which was less than the original minimum change in distance required. The system correctly identified this was the case and used the bypass value for a_r and the computed t_M and t_D from that value. Had this system used the first maneuver's a_r it is possible that a third maneuver would have been required. Also, it should be noted that for simplification and testing safety, each maneuver simulation was given 24 hours to complete and evaluate before beginning the next maneuver. With further work the simulation could be designed to begin the next maneuver one orbital period after the first maneuver is completed.

A second scenario was also tested. In this case, the satellites begin from the same initial state space as before, but now the desired change in distance was -3000 meters. Fig. 19 is the result of this maneuver.

For this case, the original maneuver overshoots the desired target. This time the satellite performs the same

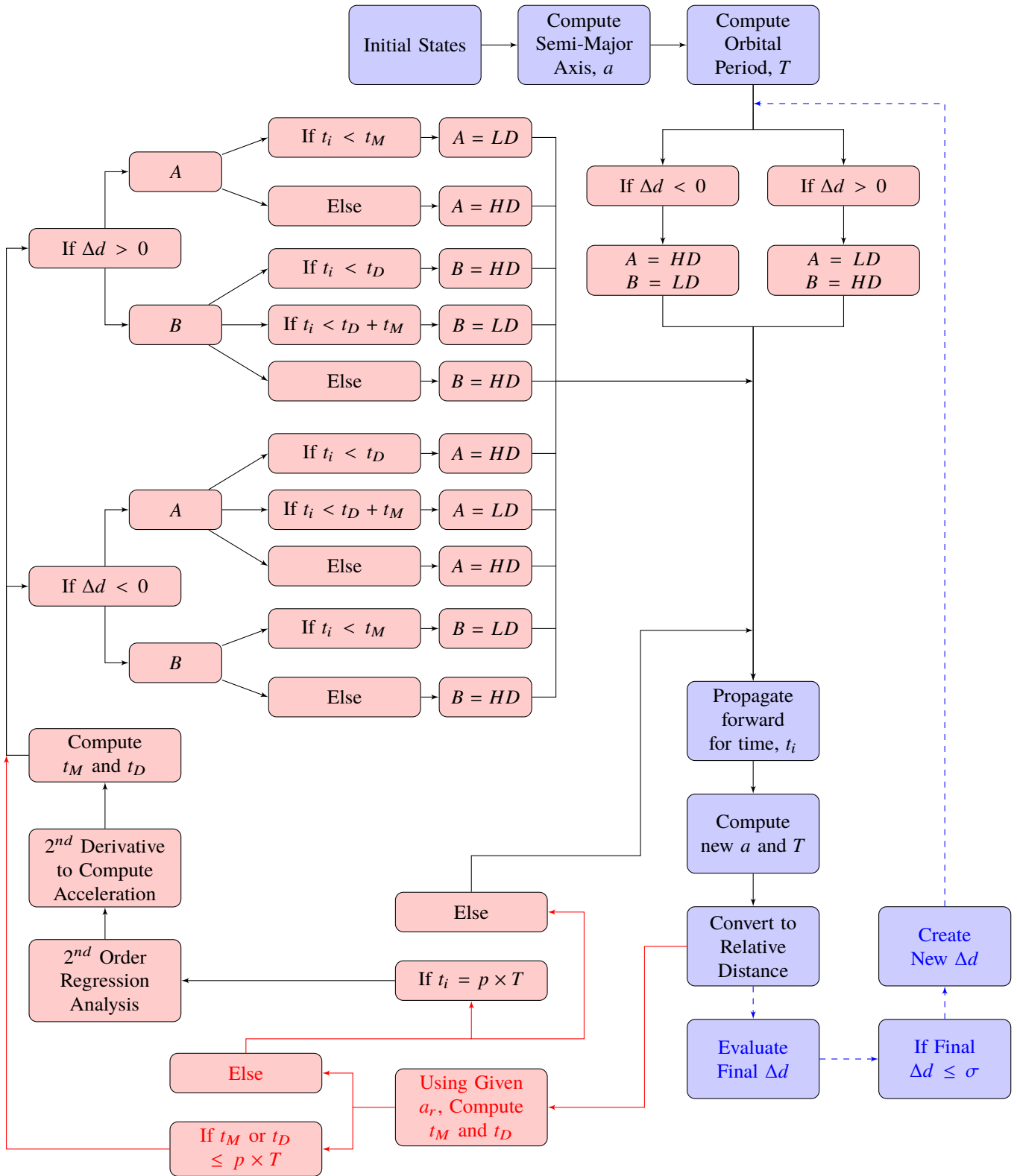


Fig. 17 Modified Distance Maneuver System

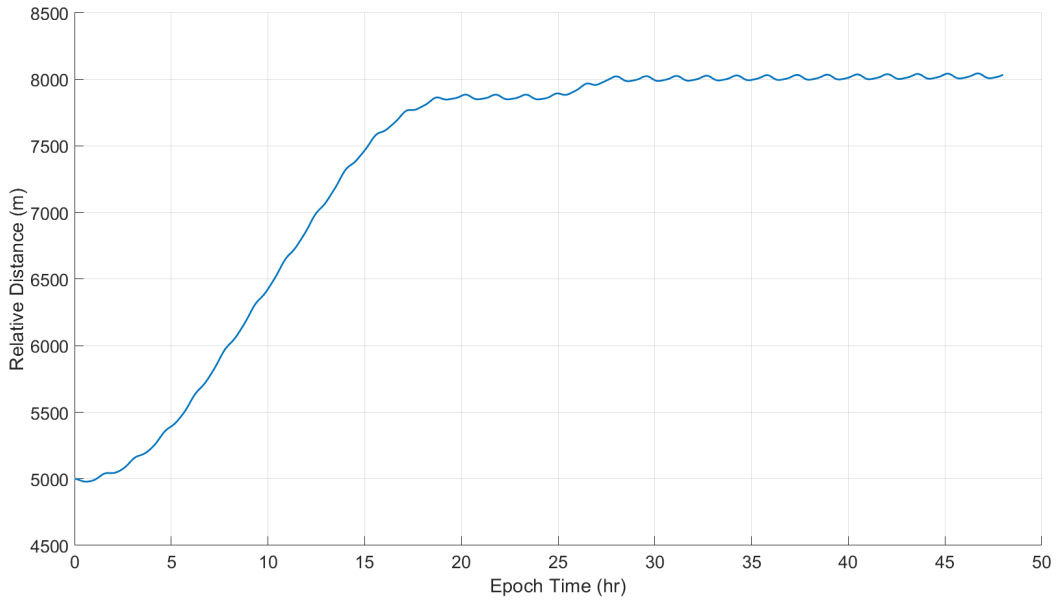


Fig. 18 3000 Meter Distance Maneuver with the Modified System

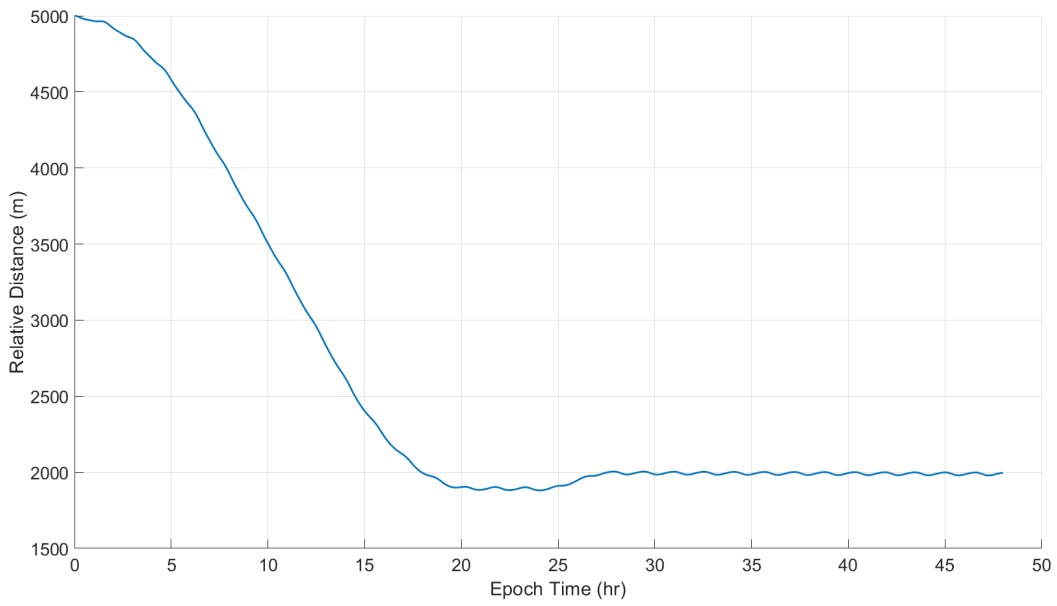


Fig. 19 -3000 Meter Distance Maneuver with the Modified System

calculations and decides it needs a positive change in distance. This change in distance is again below the minimum, so the system uses the user supplied a_r and the computed t_M and t_D associated with it. Had this second change in distance needed to be negative the system would have used the value computed for a_r in the negative case, computed as $-2.5205 \times 10^{-6} m/s^2$ in Section IV.B. The end of the second maneuver again achieves the desired final change in distance.

V. Conclusions

CubeSats continue to be an ever growing part of the spacecraft industry. With parts becoming cheaper and smaller, these satellites become easier to build. Similarly, it is easier to launch a small sat with the advent of ride-shares and small sat launchers being mounted to more and more rockets. As this section of the industry becomes more populated, more research is being done in relation to how to use CubeSats. Many different researchers have developed new control theories and uses for spacecraft rendezvous and spacecraft constellations. This paper has demonstrated a new technique for controlling identical satellites without onboard propellant through the use of differential drag.

The first new controller deals with overcoming relative distance drift between satellites. A system was developed that would take positioning data, and based on the assumption of inter-satellite communication, would change the satellites' orientations in order to arrest any drift that fell outside of a user defined allowable error. Using this system, multiple scenarios were run with variable allowable errors and different orbital period multiples used to take measurements of mean orbital periods. From this study, it was found that for the RANGE satellites, values of 0.0010 s allowable error and one orbital period multiple were ideal. Depending on the priority of the mission parameters, other orbital period multiples could be used, as long as they are greater than one. The increase in this value will add secondary oscillations to the relative distance, but will also reduce the frequency the satellites will need to change their orientation.

The other unique contribution for this paper is the use of multiple satellite maneuvers done in tandem in order to change the mean relative distance between satellites. A controller system was developed for this case. It uses quadratic polynomial regression to calculate the satellites' relative acceleration, which is then used to calculate the time period that the maneuvers should be performed for, and how long to delay the maneuver start for the other satellite. Under simulation testing, two challenges in the original system were discovered. To overcome a minimum distance limitation, a bypass was added that would use a predetermined relative acceleration rate for the maneuver time calculations. This value could either be set prior to launch or could be calculated from the satellites performing distance maneuvers that are larger than the minimum distance and then stored for later use. To overcome the offset that could be incurred due to computation error from the regression analysis, a second closed loop was added that would evaluate the mean distance between the satellites after each maneuver was performed. This loop would continue until the final mean distance fell within a user defined error tolerance.

These two systems could be used with identical satellites that will fly in formation. The automated controls are easily adaptable to real world situations and for other errors that may appear. Additionally, the MATLAB code was designed in such a way that adding higher fidelity to the orbit propagator would be easy to accomplish. This would allow more accurate predictions based on improved atmospheric models, rarefied flow analysis, 3rd body perturbations, or solar radiation pressure.

VI. Acknowledgements

This research was supported in part by the U.S. Office of Naval Research under award number N00014-16-1-2167

References

- [1] Leonard, C., Hollister, W., and Bergmann, E., "Orbital formationkeeping with differential drag," *Journal of Guidance, Control, and Dynamics*, Vol. 12, No. 1, 1989, pp. 108–113.
- [2] Mishne, D., "Formation control of satellites subject to drag variations and J2 perturbations," *Journal of Guidance, Control, and Dynamics*, Vol. 27, No. 4, 2004, pp. 685–692.
- [3] Horsley, M., "An investigation into using differential drag for controlling a formation of CubeSats," Tech. rep., Lawrence Livermore National Lab.(LLNL), Livermore, CA (United States), 2011.
- [4] Kumar, B. S., Ng, A., Yoshihara, K., and De Ruiter, A., "Differential drag as a means of spacecraft formation control," *IEEE Transactions on Aerospace and Electronic Systems*, Vol. 47, No. 2, 2011, pp. 1125–1135.

- [5] Finley, T., Rose, D., Nave, K., Wells, W., Redfern, J., Rose, R., and Ruf, C., “Techniques for leo constellation deployment and phasing utilizing differential aerodynamic drag,” *Arbor*, Vol. 1001, 2013, pp. 48109–2143.
- [6] Ben-Yaacov, O., and Gurfil, P., “Stability and performance of orbital elements feedback for cluster keeping using differential drag,” *The Journal of the Astronautical Sciences*, Vol. 61, No. 2, 2014, pp. 198–226.
- [7] Boshuizen, C., Mason, J., Klupar, P., and Spanhake, S., “Results from the planet labs flock constellation,” 2014.
- [8] Foster, C., Mason, J., Vittaldev, V., Leung, L., Beukelaers, V., Stepan, L., and Zimmerman, R., “Constellation phasing with differential drag on planet labs satellites,” *Journal of Spacecraft and Rockets*, Vol. 55, No. 2, 2017, pp. 473–483.
- [9] Varma, S., and Kumar, K. D., “Multiple satellite formation flying using differential aerodynamic drag,” *Journal of Spacecraft and Rockets*, Vol. 49, No. 2, 2012, pp. 325–336.
- [10] Kumar, K. D., Misra, A. K., Varma, S., Reid, T., and Bellefeuille, F., “Maintenance of satellite formations using environmental forces,” *Acta Astronautica*, Vol. 102, 2014, pp. 341–354.
- [11] Frey, G. R., Petersen, C. D., Leve, F. A., Garone, E., Kolmanovsky, I. V., and Girard, A. R., “Parameter governors for coordinated control of n-spacecraft formations,” *Journal of Guidance, Control, and Dynamics*, Vol. 40, No. 11, 2017, pp. 3020–3025.
- [12] Pérez, D., and Bevilacqua, R., “Lyapunov-based adaptive feedback for spacecraft planar relative maneuvering via differential drag,” *Journal of Guidance, Control, and Dynamics*, Vol. 37, No. 5, 2014, pp. 1678–1684.
- [13] Anderson, K., and Bevilacqua, R., “Propellant-free Spacecraft Relative Maneuvering via Atmospheric Differential Drag,” Tech. rep., Rensselaer Polytechnic Institute TROY United States, 2015.
- [14] Pérez, D., and Bevilacqua, R., “Differential drag-based reference trajectories for spacecraft relative maneuvering using density forecast,” *Journal of Spacecraft and Rockets*, Vol. 53, No. 1, 2016, pp. 234–239.
- [15] Di Mauro, G., Bevilacqua, R., Spiller, D., Sullivan, J., and D’Amico, S., “Continuous maneuvers for spacecraft formation flying reconfiguration using relative orbit elements,” *Acta Astronautica*, Vol. 153, 2018, pp. 311–326.
- [16] Bevilacqua, R., and Romano, M., “Rendezvous maneuvers of multiple spacecraft using differential drag under J2 perturbation,” *Journal of Guidance, Control, and Dynamics*, Vol. 31, No. 6, 2008, pp. 1595–1607.
- [17] Harris, M. W., and Açıkmüşe, B., “Minimum time rendezvous of multiple spacecraft using differential drag,” *Journal of Guidance, Control, and Dynamics*, Vol. 37, No. 2, 2014, pp. 365–373.
- [18] Dell, L., Kerschen, G., et al., “Optimal propellantless rendez-vous using differential drag,” *Acta Astronautica*, Vol. 109, 2015, pp. 112–123.
- [19] Ben-Yaacov, O., Ivantsov, A., and Gurfil, P., “Covariance analysis of differential drag-based satellite cluster flight,” *Acta Astronautica*, Vol. 123, 2016, pp. 387–396.
- [20] Mazal, L., Perez, D., Bevilacqua, R., and Curti, F., “Rendezvous via differential drag with uncertainties in the drag model,” *Proceedings of the AIAA/AAS Astrodynamics Specialist Conference, Vail, Colorado*, 2015.
- [21] Mazal, L., Pérez, D., Bevilacqua, R., and Curti, F., “Spacecraft rendezvous by differential drag under uncertainties,” *Journal of Guidance, Control, and Dynamics*, 2016, pp. 1721–1733.
- [22] Groesbeck, D. S., Hart, K. A., and Gunter, B. C., “Simulated Formation Flight of Nanosatellites Using Differential Drag with High-Fidelity Rarefied Aerodynamics,” *Journal of Guidance, Control, and Dynamics*, 2018, pp. 1–10.
- [23] Gunter, B. C., Davis, B., Lightsey, G., and Braun, R. D., “The Ranging and Nanosatellite Guidance Experiment (RANGE),” 2016.
- [24] Vallado, D., and McClain, W., *Fundamentals of Astrodynamics and Applications*, Space Technology Library, Springer Netherlands, 2001.
- [25] Curtis, H. D., *Orbital Mechanics for Engineering Students*, 3rd ed., Butterworth-Heinemann, 2013.
- [26] Hart, K. A., Simonis, K. R., Steinfeldt, B. A., and Braun, R. D., “Analytic Free-Molecular Aerodynamics for Rapid Propagation of Resident Space Objects,” *Journal of Spacecraft and Rockets*, Vol. 55, No. 1, 2017, pp. 27–36.